GeoEarthScope

LiDAR Working Group Report

September, 2006

GeoEarthScope LiDAR Working Group

Report of Working Group Task to Define and Prioritize LiDAR (ASLM) Targets for GeoEarthScope

Prepared for:
Earthscope Program
National Science Foundation

Report Prepared by:

Kevin P Furlong (Penn State University),
Chair of Working Group

Ron Bruhn, (University of Utah)
Doug Burbank, (UC Santa Barbara)
James Dolan, (Univ. Southern Cal.)
John Oldow, (Univ. of Idaho)
Charlie Rubin, (Central Washington)
Carol Prentice, (USGS-Menlo Park)
Brian Wernicke, (Cal Inst Tech)
Steve Wesnousky, (Univ. Nevada, Reno)

GeoEarthScope LiDAR Working Group
Acquisition Targets

1. Summary

LiDAR acquisition is a key component of the GeoEarthScope Initiative. It will provide data with a range of applications that will advance many of the EarthScope goals. A working group was convened to identify primary targets for data acquisition, rank these targets, and proposes a data acquisition scheme to effectively acquire these data within the GeoEarthScope funding time frame. Identified targets are grouped both geographically and within each region ranked by priority. Priority 1 targets represent those deemed critical to the GeoEarthScope goals, while Priority 2 and 3 targets are considered important but within the extremely tight funding conditions of GeoEarthScope can be considered secondary.

2. The Regional Targets are:

a. Northern California – including the San Andreas Fault north of Parkfield, and other major strands of the San Andreas Fault system (e.g. southern Hayward, Rodgers Creek, Ma'acama, etc. Faults)
   Proposed Priority 1 Data Acquisition: ~ 1370 km^2

b. Southern California – including the Garlock Fault, Eastern California Shear zone south of the Garlock, the Elsinore Fault, and regions of the transpressional faulting in the Transverse Range region. Large segments of the San Andreas and San Jacinto faults have previously acquired LiDAR as part of the B4 project.
   Proposed Priority 1 Data Acquisition: ~ 1953 km^2

c. Eastern California, Walker Lane, and Basin and Range fault systems – including faults of the Eastern California Shear Zone north of the Garlock Fault.
   Proposed Priority 1 Data Acquisition: ~ 2010 km^2

d. Intermountain Seismic Belt – including the Wasatch Fault, Teton Fault, Yellowstone Park area, and northern extensions of the system through Idaho and Montana.
   Proposed Priority 1 Data Acquisition: ~ 1513 km^2

e. Alaska – including the Castle Mountain and Denali Faults, and the Nenana River terraces.
Proposed Priority 1 Data Acquisition: ~ 540 km^2

f. Cascadia – including the Mad River and Little Salmon fault zones in southern Cascadia, the Calawah Fault in the Washington forearc, and imagery in the Yakima Fold belt termination.
Proposed Priority 1 Data Acquisition: ~ 550 km^2

TOTAL Proposed Priority 1 Data Acquisition: ~ 7936 km^2

Within each target region, specific faults and fault systems were identified for LiDAR data acquisition as part of GeoEarthScope; each target was ranked according to priority; and a provisional timetable was developed for acquisition with each region. The timetable considered the need for completing data acquisition during the current EarthScope funding cycle, seasonal timing for optimum data gathering in each region considering weather conditions (rain, temperature, etc) and other issues, and the perceived benefits gained from completing the northern San Andreas as soon as possible to link to the recently acquired southern San Andreas data.

3. Prioritization

Although firm budgets were not available to the group, nor were the actual costs of data acquisition fully known, total square kilometers of data acquisition were assigned to each group according to the Working Group's assessment of needs within each region. It is hoped that all Priority 1 sites and most if not all of Priority 2 sites are collected with current GeoEarthScope funding. The Working Group recognized that available funding would likely preclude obtaining data from very many of the Priority 3 sites. It should be understood that all sites identified – including Priority 3 sites – had the full support of the Working Group, and the relative rankings were made with some very hard choices among those sites.

In the body of this report the targets in each region are identified, total estimated square kilometers of data acquisition are provided, and sites are ranked within regions. All regions were considered key parts of Geo EarthScope and the Working Group made its decisions based on the assumption that all regions will have substantial data acquisition efforts as part of the current funding.

4. Background Issues

The Working Group wrestled with several important issues that affect the data acquisition plan and the prioritization of sites. We recognized we were working with a limited resource in terms of available funding, and the WG tried to develop

a plan that honored the primary EarthScope goals. This was not an easy task, and the results are a plan embraced by the WG; but also seen realistically as a first step in a continuing need for LiDAR data acquisition in the PBO region. In particular, in order to maximize the coverage obtained and serve the broadest community, the WG elected to utilize relatively narrow swath widths (typically 1 km, widened to 2+km in key regions), which allowed more line-kilometers of data to be obtained. The unavoidable consequences of this choice are that areas away from the main fault strands will be unsampled, more complex flight lines may be necessary, and the usefulness of the data obtained in this initial acquisition may have more limited value to researchers interested in non-fault specific topics. It is hoped that this data set will be augmented in the future with targeted data acquisition that mitigates these shortcomings.

In the following discussions of each region, the rationale for specific swath widths, broader 'boxed' regions, and other targets are described. It is recommended that as each target regions data acquisition is planned, that one or more members of the WG be involved with UNAVCO personnel to define details of the data acquisition.

5. Logistics

The WG also discussed logistical details of data acquisition. They recognized the importance of obtaining high-quality data that will be valuable for years to come. Some questions were raised about the need for what was termed 'B4 ground control' for all sites. It was thought that in many areas it would be both impractical and perhaps unnecessary to such stringent constraints on ground station spacing etc.

In order to better assess this question, it was decided that as part of the first data acquisition in northern California, that the section of the San Andreas from Fort Ross to Point Arena would be re flown as part of this data acquisition. A broader swath was previously obtained by other funding sources with 'less than B4 ground control'. In this way we (we being the Working Group) will be able to assess the data improvements from B4 style acquisition in advance of the rest of the data gathering. In order for the GeoEarthScope project to benefit from this comparison this region of the fault will be the highest priority for acquisition and processing so informed decisions can be made for the later data acquisition.

The WG had no strong feelings about the choice of contractor for data acquisition. It was comfortable with the following methodology for sub-awards:

- NCALM – airborne laser scanning (although other groups would be acceptable
- OSU – GPS heavy ground control services (their expertise with B4 would provide continuity)

- ASU – data distribution services (GEON LiDAR workflow type distribution)
- UNAVCO will provide archiving services and support for GPS ground control in addition to project management.

6. Proposed Timetable

The following reflects the proposed timetable for data acquisition, based on balancing priorities including optimal times for data collection in each region, and meeting the GeoEarthScope deadlines of completion by Summer 2008.

Fall 2006
Northern California

Spring 2007
Southern California

Late summer/Fall 2007
Intermountain Seismic Belt, including Yellowstone

Spring 2008
Eastern California Shear Zone,
Basin & Range, Walker Lane (May or June)

Summer 2008
Alaska, Cascadia

7. Working Group

Members of the Working Group and their affiliations are given below. Several members of the UNAVCO staff also participated in the meeting, providing information as requested by the Working Group. They are thanked for their very important contributions.

GeoEarthScope LiDAR (ASLM) Working Group

Kevin Furlong, Penn State (Chair of Working Group)
Ron Bruhn, University of Utah
Doug Burbank, UC Santa Barbara
James Dolan, USC
John Oldow, U of Idaho
Charlie Rubin, Central Washington
Carol Prentice, USGS
Brian Wernicke, Cal Tech
Steve Wesnousky, University of Nevada, Reno

UNAVCO Personnel in attendance at Working Group Meeting

Will Prescott	Chuck Meertens	David Phillips
Mike Jackson	Jaime Magliocca	

Additional Notes on Report:

i. *Final report was assembled and edited by K.P. Furlong. He takes full responsibility for all errors in this document.*

ii. *Details of the report format (for each target region) vary to most efficiently convey issues related to that region.*

iii. *Rather than provide incomplete citation and referencing, in this report we have elected to provide minimal citations. As an internal document meant primarily for planning purposes, the WG felt this was an appropriate approach.*

Northern California – Northern San Andreas Plate Boundary System

Overview of Region

Approximately 70% of the total plate boundary motion is accommodated across a less than 100-km-wide region in northern California. The nine counties that comprise the greater San Francisco Bay area, population approximately seven million, lie within this region, making this system of faults among the most important in the US in terms of seismic hazard. The intense forest cover that blankets much of this region has hampered detailed study of these faults, making LiDAR data an especially useful tool.

Details of the Fault System

Near the southern end of the region, at least half of the plate-boundary motion (25-30 mm/yr out of approximately 50 mm/yr) is concentrated along a single fault, the creeping section of the San Andreas Fault north of Parkfield. However, this situation changes dramatically north of the latitude of Hollister, where this single fault becomes a complex system of strike-slip and reverse faults that traverses the San Francisco Bay region, and continues northward to the latitude of the Mendocino Triple Junction. From the San Francisco Bay area northward to the subduction zone transition, most of the San Andreas motion is taken up by eight principle strike-slip faults: the San Andreas, San Gregorio, Hayward, Rodgers Creek, Maacama, Calaveras, Concord-Green Valley, and Bartlett Springs fault zones. In addition, a number of blind thrusts and reverse faults accommodate contractional motion in the region.

Targets

We have identified 26 target regions within northern California, and have assigned them to priority categories 1, 2, or 3 (Table 1, Figure 1). A total of approximately 1370 km^2 is designated priority 1. The San Andreas Fault north of Parkfield to its northern end near Shelter Cove is considered a particularly high priority.

Special Considerations

Northern California's climate is considerably wetter than that of southern California, and therefore the landscape in many parts of the region is covered with dense forest, especially near the coast. This gives rise to some special considerations in planning a LiDAR acquisition program along major active faults. In many areas, the locations of the principal faults are not well enough defined to be confident that a one-km wide swath will contain the main fault trace. In addition, in many areas, bends and steps give rise to structural complexities that are best studied by collecting data within a broader region rather than a simple one-km-wide swath along one particular fault. For this reason, we have identified 11 areas where regions wider than one km are necessary. Three of these are associated with the San Andreas Fault, and two additional are designated as priority 1 targets.

Other Points to Consider

We have omitted most of the Hayward and Concord faults because they are in highly urbanized areas where LiDAR will be less useful for fault studies. The zones where we propose swaths that are wider than one-km-wide are each unique. Along the San Andreas Fault, the Santa Cruz Mountains region (55 km long) is proposed as a two-km-wide swath because its location is poorly known and the fault zone through this region is wide and complex due to the Loma Prieta bend. Farther south, we propose a 3-km-wide swath along the southern creeping section to include Mustang Ridge, a prominent pressure ridge in a constraining stepover and the complex and wide fault zone south of there, including the SAFOD drill site. The creeping section has recently become a section of interest due to new GPS geodetic studies that suggest the creep rate across the main trace is only about 25 mm/yr, significantly less than the 34 mm/yr for the long-term geologic rate in the Carrizo Plain, suggesting that either there are subsidiary active traces parallel to the main trace or that strain is accumulating along this fault segment.

In addition, we propose a two-km-wide swath along the central Calaveras because the fault is wide and complex in the region of its interaction with the southern Hayward Fault. We have included (as a Priority 1 target) a 5-km (N-S extent) east-west swath starting at the Coast near Shelter Cove and extending across all of the known strike-slip faults. This region is within the transition zone from the transform plate margin to the Cascadia subduction zone and is heavily forested, difficult terrain. The purpose of this swath is to determine whether additional structures are present that accommodate some of the plate motion, and whether the topography is indicative of distributed deformation in this region. Additionally a second short 1 km wide swath has been selected along the Maacama Fault system from Calpella at south end of Redwood Valley) along the east side of the Laughlin Range and east side of Little Lake Valley. Along this swath geophysical evidence suggest a secondary trace of the fault that parallels the well documented creeping trace through Willits.

There are three prominent stepover regions where we have proposed (as Priority 2 targets) imaging larger regions in order to better understand how slip is transferred between the faults. These are the San Andreas-Calaveras junction (Box D), the Calaveras-Hayward stepover (Box B) and the Rodgers Creek-Maacama stepover (Box C). As priority 3 targets, we have included the West Napa, Bartlett Springs, and Paicines faults as 2-km-wide swaths because of their complexity and poorly mapped surface traces. Finally, we have included a region near Winters to better understand the active folding and blind thrusting in the area adjacent to the Delta and its seismically vulnerable levees.

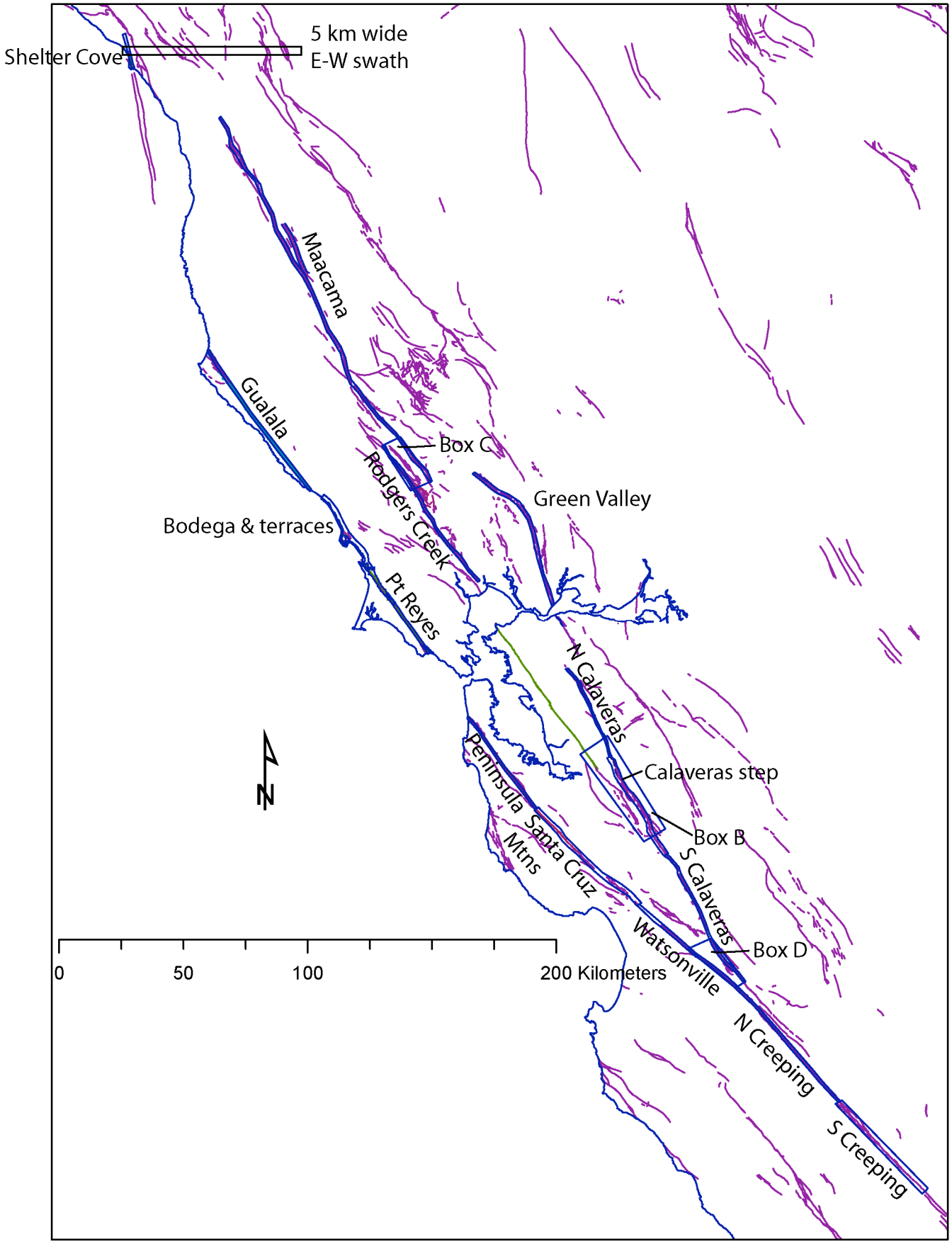
5 km wide
E-W swath
Shelter Cove
Maacama
Gualala
Box C
Rodgers Creek
Green Valley
Bodega & terraces
Pt Reyes
N Calaveras
Calaveras step
Box B
Peninsula
Santa Cruz
Mtns
S Calaveras
Watsonville
Box D
N Creeping
S Creeping
N
0
50
100
200 Kilometers

Northern California Target Areas

I. San Andreas Fault from northern end of B4 project to Shelter Cove 595 km^2 Listed from north to south

Priority	Name	Fault length (km)	Preferred swath width (km)	Area km^2	Cumulative total area km^2	comments
1	Shelter Cove	15 km	1	15	15	
1	Gualala	70	1	70	85	Redo exisiting
1	Bodega		2	70	155	Marine terraces & short fault section
1	Point Reyes	30	1	30	185	Includes Millerton Point
1	SF Peninsula	40	1	40	225	
1	Santa Cruz Mountains	55	2	110	335	
1	Watsonville	30	1	30	365	
1	Northern Creeping	80	1	80	445	
1	Southern Creeping	50	3	150	595	Mustang Ridge stepover and SAFOD

II. Other northern California strike-slip faults ~ 500 km^2 Listed in order of priority

Priority	Name	Fault length (km)	Preferred swath width (km)	Area km^2	Cumulative total area km^2	comments
1	Green Valley	70	1	70	665	
1	Rodgers Creek	65	1	65	730	
1	S Calaveras	60	1	60	790	
1	Calaveras step	45	2	90	880	Fault complex and wide
1	N Calaveras	40	1	40	920	
1	Maacama	150 + 25	1	175	1095	

III. Regions 930 km^2 Listed in order of priority

Priority	Box number	Name	Preferred swath width (km)	Area km^2	Cumulative total area km^2	comments
1	A	Shelter Cove to Bartlett Springs	5	300	1370	SW-NE swath 5 km wide
2	B	Calaveras-Hayward Stepover		360	1730	
2	C	Rodgers Creek-Maacama stepover		150	1880	
2	D	San Andreas – Calaveras stepover		120	2000	

Other faults and regions Listed in order of priority

Priority	Name	Length (km)	Preferred swath width (km)	Area km^2	Cumulative total area km^2	comments
3	West Napa	35	2	70	2070	
3	Greenville	60	1	60	2130	
3	Paicines	30	2	60	2160	Included in Box D
3	San Gregorio			300	2560	Includes both strands and marine terraces from S of Año Nuevo to N of Half Moon Bay
3	Bartlett Springs	150	2	300	2860	
3	Rinconada	130	1	130	2990	
3	Winters fold			100	3090	Blind thrust

Southern California

Overview of Region

We define two sets of high-priority LiDAR targets in southern California. One set focuses on several of the largest, fastest-slipping strike-slip faults in the region, including the Garlock fault, the faults of eastern California shear zone (ECSZ) in the Mojave region, and the Elsinore fault. Acquisition of these targets will complement the recently acquired "B4" data set. The second set focuses on thrust faults, both surface-rupturing and blind, that predominate within the Transverse and Coast Ranges. Together, these data sets will not only characterize the high-resolution topography along many of the major faults that make up the Pacific-North America plate boundary in southern California, but they will capture the local geomorphologic conditions that record responses to deformation and modulate many surface processes in catchments crossing faults.

Targets (Table 2)

The first two major strike-slip targets also lie at the heart of the geodetic-geologic mismatch controversy. For the Garlock fault, the geologic rates are more rapid than the geodetic rates, whereas the opposite appears to be true for the Eastern California Shear Zone (ECSZ). The Garlock fault is a major left-lateral fault extending 240 km eastward from its intersection with the San Andreas Fault (SAF). Interestingly, although geological studies indicate that the Garlock's latest Pleistocene-Holocene slip rate is ~6-9 mm/yr, short-term geodetic studies suggest that the current rate of strain accumulation across the fault is occurring much more slowly, on the order of only a few mm/yr. Resolution of this discrepancy is a major motivation for future research along the Garlock fault.

The right-lateral faults of the ECSZ in the Mojave Desert may also represent a "strain transient". Short-term geodetic data indicate elastic strain accumulation at a rate of ~12 mm/yr across this set of faults. In contrast, geological studies of longer-term slip rates suggest that strain release across this system is considerably slower than 12 mm/yr. The proposed acquisition of LiDAR swaths along all of these major faults will greatly facilitate future research into this interesting geodynamical question.

The mechanisms by which differential motion at high angles to strike-slip faults is transferred across them remains unresolved. Deformation in the northeastern part of the Mojave section of the ECSZ is accommodated by both vertical axis rotations and slip on east-west left-lateral faults. We propose to collect LiDAR data along the major left-lateral faults in order to fully characterize deformation in the ECSZ, and to understand how plate-boundary motion is transferred from the southern ECSZ, across the Garlock fault, and onto the major faults of the northern part of the ECSZ (Panamint-Hunter Mountain fault and Death Valley-Fish Lake Valley fault system [discussed in the Walker Lane region]).

The final of our strike-slip target is the Elsinore fault, which extends for >200 km from the southeastern edge of the Los Angeles metropolitan region to the Mexican border. This right-lateral fault may accommodate ~10% of total relative plate motion in southern California.

LiDAR data has already been collected across the San Andreas proper and its other major splay, the San Jacinto fault, as part of the B4 project. Collection of a similar data set along the length of the Elsinore fault will thus provide a complete data base for the three fastest-slipping strands of the right-lateral plate boundary fault system.

Other Points to Consider

Outside of subduction zones, the highest rates (~10 mm/yr) of contractional deformation in the conterminous US occur in the Transverse Ranges. Some of the thrust faults accommodating this shortening are blind, and several bound major metropolitan areas where they pose an enormous seismic hazard. These faults are also interesting because, unlike strike-slip faults, deformation on thrust faults strongly modulates geomorphic base level and hence exerts controls on the geomorphic development of upstream catchments. We, therefore, target several large, rapidly slipping reverse faults in the Transverse Ranges and Coast Ranges contractional systems. Specific targets include: (1) the north-dipping San Cayetano and south-dipping Oak Ridge faults bounding the Ventura basin (the 1994 Mw 6.7 Northridge earthquake is thought to have occurred on a previously unrecognized splay of the easternmost Oak Ridge fault system); (2) the Sierra Madre-Cucamonga thrust system that bounds the Los Angeles basin along the southern San Gabriel mountains; (3) the south-dipping North frontal fault along the northern edge of the San Bernardino mountains; (4) the Pleito Thrust system in the San Emigdio Mountains along the southern edge of the San Joaquin Valley (the White Wolf fault, a major splay in the eastern part this thrust system, generated the 1952 Mw 7.5 Kern County earthquake); and (5) the multiple blind thrust faults of the Coalinga-Kettleman Hills region along the western edge of the San Joaquin Valley (these faults generated a series of moderate-magnitude earthquakes during the 1980s, including the 1983 M_w 6.5 Coaling earthquake). Each of these target areas will provide important new data on the geomorphologic and structural development of the folds that form above these thrust faults, as well as vitally important information concerning the seismic hazards that these faults present.

Table 2. Southern California

Region	Fault	Priority	LiDAR Area (km^2)
Garlock-Transverse Ranges			
	Garlock	1	600 (300 x 2 km wide swath)
	San Cayetano	1	25
	Oak Ridge	1	30
	Cucamonga-Sierra Madre	1	180 (115 length ~ ½ at 2 km swath)
	Elsinore	1	240
	Sub-Total		*1075 km^2*
ECSZ – South of Garlock Fault			
	Hellendale	1	128
	Lenwood	1	150
	Camp Rock – Homestead	1	100
	Calico	1	90
	Blackwater	1	90
	Bullion	1	90
	Pisgah	1	90
	Manix – Bicycle Lakes	1	140
	Sub-Total		*878 km^2*
Total			***1953 km^2***

Walker Lane and Basin & Range Elements of the Plate Boundary

Overview of Region

Pacific-North American relative plate motion at the latitude of the San Andreas fault system is ~50 mm/yr [*DeMets and Dixon*, 1999]. While the transform motion is taken up largely on the San Andreas fault system, upwards of 25% the relative plate-motion is accommodated by strike-slip and normal faults that lie to the east of the Sierra Nevada and which are distributed across the ~800km Great Basin physiographic province. The deformation is taken up primarily along a discontinuous set of northwest trending strike-slip faults that mark an ~80-100 km wide zone along the eastern edge of the Sierra Nevada referred to as the Walker Lane. A lesser amount of the displacement is diffusely distributed across the Great Basin along northerly-striking normal faults that constitute the Basin and Range physiography. The Plate Boundary Observatory (PBO) has designed a GPS array to capture the characteristics of strain accumulation across the Great Basin. The planned acquisition of LIDAR imagery is planned to directly compliment the PBO deployment. The targets of acquisition are primarily the major faults lying along an east-west transect of PBO GPS sites that cross the Great Basin.

The motivation to establish this archive of images are 1) to allow assessment of longer term rates of fault displacement which may be compared to modern geodetic measurements, 2) to provide an initial data base for a wide spectrum of geologists to study of the processes attendant to the structural, physiographic, and geomorphic development of the Great Basin that results from the release of the ongoing accumulation of strain that is measured by PBO, 3) to document the slip character of historical earthquakes, and 4) provide an archive of images of sites that may be the locus of future earthquake displacements.

Competing interests and funding limit the planned acquisition to about 2000 km^2 of imagery. The target faults are shown in Figure 2 and the respective line lengths of acquisition are listed in Table 3. The values of fault length to be flown listed in Table 3 assume a 1-km wide swath of LiDAR coverage. Highest priority faults are color coded in Figure 2. Faults within the Walker Lane are red, normal faults across the interior of the Great Basin are pink, and historical earthquake ruptures are yellow. Faults currently listed as 2^{nd} priority are colored blue and faults already in the stages of collection are green. Targets in the Walker Lane (red lines) are chosen to provide coverage of faults considered to be most active and accommodating the majority of strike-slip motion in the Walker Lane. The line of targets across the Basin and Range (pink lines) is taken to include the major normal fault-bounded range fronts along the densest proposed line of GPS receivers to span the Great Basin. About 500 km^2 of acquisition is allocated for the Basin and Range normal faults which equates to about 30 km per fault on average. Hence, it is not intended to fly the entirety of each fault and there will likely be a redistribution of the line length associated to particular flights closer to the time of the mission. Refinement of lines will benefit from investigators working in the region. It is intended to focus flight lines along those portions of the faults that most interact with and are confined within Quaternary deposits and mostly avoid the collection of sites where faults mark a bedrock-alluvial contact. There are few examples of historical normal surface-rupture earthquakes. As such, it is viewed high priority to collect imagery along these faults to better understand the morphological expression and slip characteristics of normal slip earthquakes.

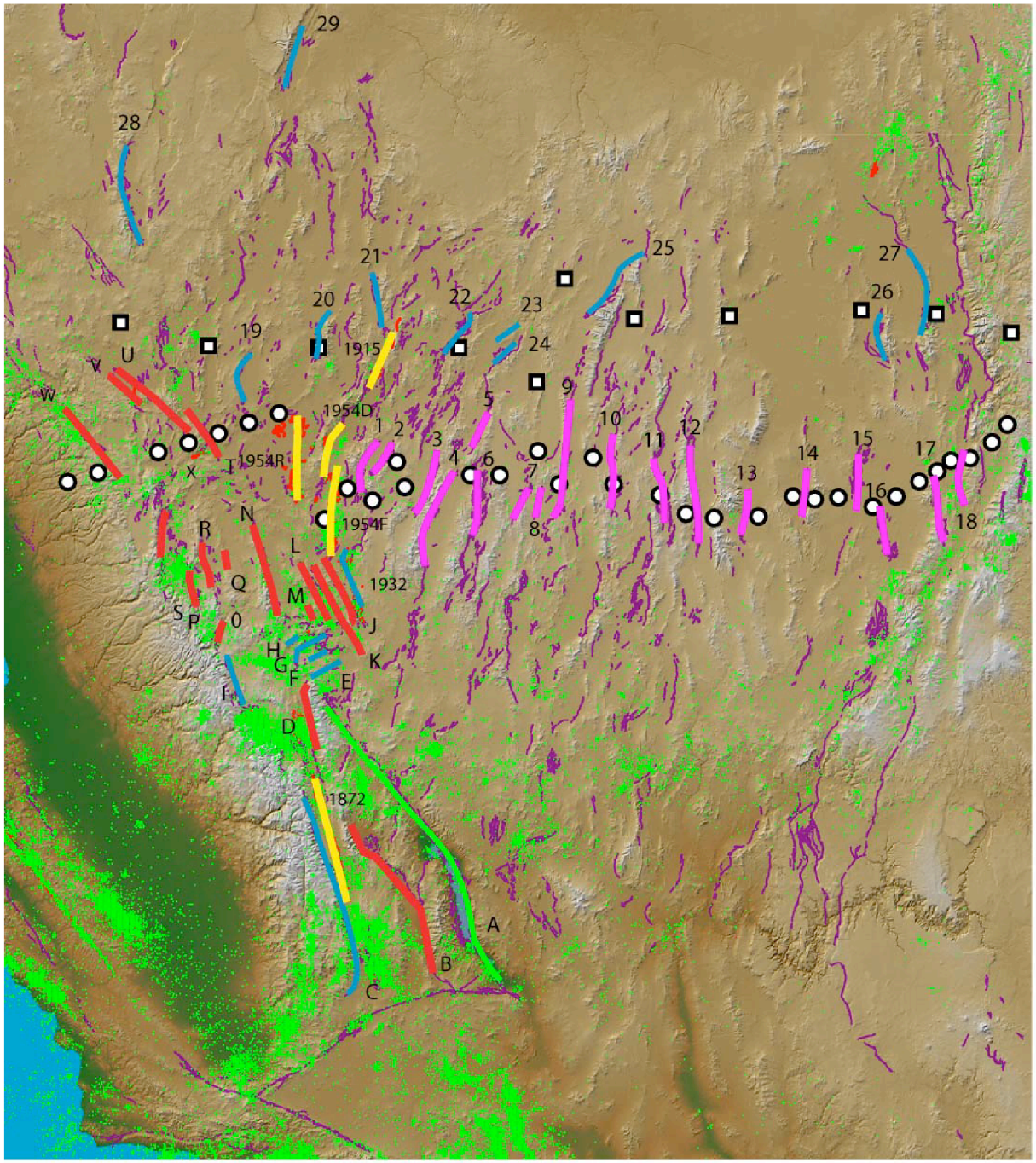

Basin & Range I-50 Transect

1. Clan Alpine
2. Desatoya
3. Toiyabe E.
4. Toiyabe W.
5. Simpson Park
6. Toquima
7. Monitor W.
8. Monitor E.
9. Diamond
10. Butte
11. Egan
12. Schell Creek
13. Snake Range
14. Utah - House Range
15. Utah - Drum Mountains
16. Utah - Clear Lake
17. Utah - Scipio-Little Valley
18. Utah - Wasatch - Levan

Basin & Range I-80 Transect

19. Shawave
20. Humboldts
21. Sonoma
22. Shoshone
23. Dry Hills
24. Cortez
25. Rubys
26. Stansbury Utah
27. E. Salt Lake Utah

Historical Earthquakes

1872 . Owens Valley
1932 . Cedar
1954 F. Fairview
1954D. Dixie
1954R. Fallon-Rainbow
1915 . Pleasant Valley

Basin & Range Northwest

28. Surprise Valley, CA
29. Steens

Walker Lane

A. Death Valley -Furnace - Fish Lake
B. Panamint-Hunter-Saline
C. South Sierra Range front
D. White Mtns
E. Coaldale
F. Candelaria
G. Teels Marsh
H. Rattlesnake
I. Mono-Hilton
J. Petrified-Bettles
K. Benton Springs
L. Gumdrop
M. Indian Head
N. Wassuk
O. Bridgeport
P. Antelope V.-Topaz
Q. Mason Valley
R. Smith Valley
S. Genoa-Carson
T. Pryamid
U. Warm Spring
V. Honey Lake
W. Mohawk Valley
X. Olinghouse

Figure Caption

Location of faults (bold color lines) planned for LIDAR acquisition on physiographic fault. Also shown in thin lines are other Quaternary faults in Region. Priority 1 faults in Walker Lane, across Basin and Range, and historical ruptures are colored red, purple, and yellow, respectively. Priority 2 faults are colored blue. Green faults are already being acquired. Dots and squares are planned distribution of PBO GPS sites across Basn and Range. Squares are locartion of current BARGEN network. Green dots are background seismicity

Walker Lane - Basin and Range Targets

Flt Number	Flt Name	Flt Length Priority 1	Flt Length Priority 2	Already Scheduled
	WALKER LANE FAULT SYSTEM			
A	Death Valley - Furnace Creek - Fish Lake Valley System			455
B	Panamint-Hunter Mountain-Saline Systme	175		
C	South Sierra Range Front		230	
D	White Mountains	110		
E	Coaldale		40	
F	Candelaria		20	
G	Teels Marsh		40	
H	Rattlesnake		20	
I	Mono Basin-Hilton Creek		25	
J	Wassuks	125		
K	Indian Head	25		
L	Gumdrop	60		
M	Benton Springs	100		
N	Petrified Springs - Bettles	50		
O	Bridgeport	30		
P	Topaz	20		
Q	Mason Valley	20		
R	Smith Valley	20		
S	Genoa	80		
T	Mohawk Valley	80		
U	Pyramid Lake	50		
V	Warm Springs	80		
W	Honey Lake	60		
X	Olinghouse		35	
	Walker Lane System total =	**1085**	**410**	
	HISTORICAL EARTHQUAKE RUPTRES			
1932	1932 Cedar Mountain Rupture		60	
1954F	1954 Fairview Peak	75		
1954D	1954 Dixie Valley	50		
1954R	1954 Fallon-Stillwater	50		
1915	1915 Pleasant Valley + stillwater gap	100		
1872	1872 Owens Valley Rupture	110		
	Historical Ruptures Total	**385**	**60**	
	BASIN & RANGE NORMAL FAULTS along PBO (Interstate 50)			
1	Clan Apline	30		
2	Desatoya	30		
3	ToiyabeW	30		
4	Toiyabe E	30		
5	Simpson Park	30		
6	Toquima	30		
7	Monitor W	30		
8	Monitor E	30		
9	Diamond	30		
10	Butte	30		
11	Egan	30		
12	Schell Creek	30		
13	Snake Range	30		

14	House Range Utah		30	
15	Drum Mountains Utah		30	
16	Clear Lake Utah		30	
17	Little Valley Utah		30	
18	Wasatch-Levan Utah		30	
		Basin & Range PBO (I50) total	**540**	**0**
	Basin & Range Normal Faults along BARGEN/I80			
19	Shawave			40
20	Humboldts			40
21	Sonoma			40
22	Shoshone			40
23	Dry Hills			40
24	Cortez			30
25	Rubys			30
26	Stansbury Utah			40
27	E. Salt Lake Utah			40
			0	**340**
	Basin & Range Northwest			
28	Surprise Valley			40
29	Steens			40
			0	**80**
		TOTAL	2010	890

Intermountain Seismic Belt LiDAR Project

Goals

Targets for LiDAR acquisition in the Intermountain Seismic Belt (ISB) focus on the geomorphology, slip-rates, and kinematics of seismogenic normal faulting, the structural and dynamic interactions between the Yellowstone volcanic hotspot and regional extension of the continental lithosphere, and the structural transition from extension to strike-slip faulting and contraction at the northern boundary of the Basin and Range Province. Specific targets are 1) the Wasatch normal fault zone in Utah, 2) the Yellowstone 'super-volcano' and adjacent Teton and Hebgen normal faults in Wyoming and Montana, 3) systems of Holocene normal faults located north of the Snake River Plain in Idaho, and 4) faults in northern Idaho and northwestern Montana where extension of continental lithosphere ends and transfers into strike-slip faults and possible contractional structures (See Figure 3, Table 4).

Geological Synopsis

The ISB is defined by a swath of earthquake activity that extends from the plate boundary in southern California northward along the transition between the Basin and Range and the Colorado Plateau and Rocky Mountains Provinces to western Montana near the Canadian border (Smith and Arabasz, 1991). The earthquake belt straddles large normal-fault bounded mountains and basins that are superimposed on earlier contractional structures of the Sevier and Laramide orogenic systems. The north-trending belt of normal faulting is disrupted by the east-trending hot spot track of the Snake River Plain, which culminates eastward in the active volcanic system at Yellowstone.

Fifty moderate-to-large magnitude (M 5.5 to 7.5) earthquakes have occurred within ISB belt since 1900, with the largest events located in the northern part of the belt. These include the M 7.5 Hebgen, MT earthquake in 1959 and the M 7.3 Borah Peak earthquake in 1983. Ground ruptures, focal mechanisms, and GPS surveys indicate regional east-west extension except where the displacement field is modified by volcanic processes at Yellowstone. Deformation rates are several millimeters per year or less on most normal faults, but increase to rates of several centimeters per year in the Yellowstone volcanic system.

Research Impacts

The normal fault and volcano system of the northern ISB provides a world-class, and in fact unique, natural setting to study the dynamics of normal faulting and the interactions between lithosphere extension and volcanism. The ISB represents the eastern limit of the broad and diffuse plate boundary of western North America, the primary target of PBO and truly an EarthScope-scale feature. The Wasatch normal fault plays a central role in theories of fault zone segmentation, and earthquake rupture behavior, placing it on par with the San Andreas fault with respect to importance in the field of paleoseismology and development of techniques for estimating earthquake hazards. Studies of the Yellowstone volcano and adjacent regions hold the promise of understanding how a lithosphere-penetrating hot spot modifies regional stresses and

deformation of the continent, including earthquake-generating faulting as well as loci of uplift and subsidence within the caldera and volcanic plateau. Other faults within the region provide opportunities to investigate how fault-bounded ranges develop and how normal faults interact both along and across the regional structural grain. In northwestern Montana and northern Idaho, the northern terminus of Basin and Range type extension is exposed and provides an unprecedented opportunity to investigate mechanisms of displacement transfer between extensional and transcurrent faults of the Lewis and Clark Shear Zone. At issue is how the transition from transform motion to subduction along the Pacific coast is reflected in the change from normal to strike-slip faulting far within the continental interior.

Geological Hazards

Although fault slip rates in the northern ISB are significantly less than those on many strike-slip faults located along the Pacific Coast, the earthquake hazard and social implications of earthquakes in the ISB are considerable (Smith and Arabasz, 1991; Quaternary fold and fault database, USGS and others, 2006). The Wasatch normal fault zone extends through the high density urban corridor of the Wasatch Front in Utah, with 2005 population in excess of 2 million people. This is the 7th largest metropolitan area in the U.S. More than 50, and perhaps as many as 120, surface rupturing earthquakes have occurred in this fault zone in the last 18 ka (Haller et al., 2005), with the most recent event around 600 years ago. The next surface rupturing earthquake will severely impact the high density population and economic infrastructure, which are growing at one of the highest rates in the U.S. Teton and Yellowstone National parks draw over 2.8 million visitors from around the globe every year, providing a unique opportunity for the earth science community to educate the general public about both volcanic and fault hazards, as how these features influence the landscape. Hazard to life and property posed by the Yellowstone super-volcano, should it erupt as it has several times in the past, will be devastating to large parts of the U.S., and also have global effects on climate. The Teton normal fault poses significant earthquake hazard to the growing population of the Jackson Hole, WY region, including also the possibility of dam failure, flooding, and disruption of irrigation for agriculture in adjacent parts of Idaho. The 1959 Hebgen Lake, MT earthquake demonstrated first-hand the potential impact of ground rupture and shaking in mountainous terrain. The earthquake triggered a gigantic rock slide that severed the road way and dammed the Madison River, creating a significant potential for catastrophic flooding that was alleviated only because of quick action on the part of government authorities. Elsewhere in the northern ISB towns and cities continue to grow even though the region is sparsely populated compared to the west coast. This should be viewed as an opportunity to take the long, instead of short, view in terms of research and planning for growth in the future. Currently we have the opportunity to locate and study active tectonic features in anticipation of further population and infrastructure growth, unlike the situation in other parts of the country where discovery and planning for natural hazards lags behind development, and where crucial geological relationships have been destroyed by urbanization.

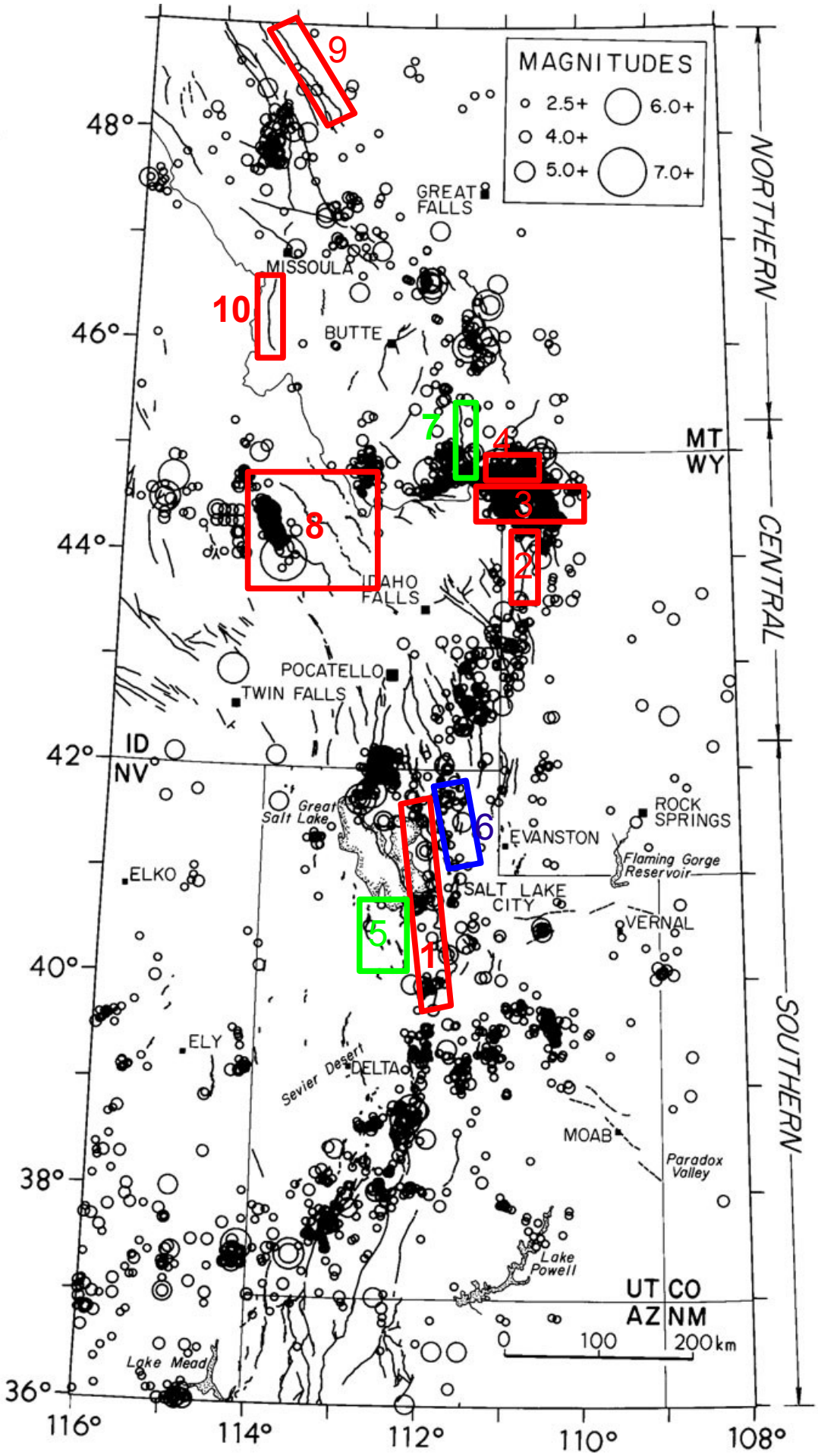
MAGNITUDES
2.5+
4.0+
5.0+
6.0+
7.0+
NORTHERN
CENTRAL
SOUTHERN
MT
WY
ID
NV
UT
CO
AZ
NM
48°
46°
44°
42°
40°
38°
36°
116°
114°
112°
110°
108°
GREAT FALLS
MISSOULA
BUTTE
IDAHO FALLS
POCATELLO
TWIN FALLS
ELKO
ELY
DELTA
Great Salt Lake
Sevier Desert
Lake Mead
EVANSTON
ROCK SPRINGS
Flaming Gorge Reservoir
SALT LAKE CITY
VERNAL
MOAB
Paradox Valley
Lake Powell
0
100
200km
1
2
3
4
5
6
7
8
9
10

Figure 3 Legend:

Fault and earthquake map of the Intermountain Seismic Belt with fault localities enclosed in numbered rectangular regions. Priority 1 faults enclosed in red, priority 2 in green and priority 3 in blue. Lewis and Clark shear zone area in northwestern Montana and northern Idaho not marked on the map.

1) Wasatch Fault, Utah, 2) Teton Fault, WY, 3) area of two east-west swaths in Yellowstone Park, 4) Hebgen Fault, MT, 5) Oquirrh and Stansbury faults, UT, 6) Cache Valley Faults, UT, 7) Madison Fault, MT, 8) Central Idaho faults – from west to east the Lost River, Lemhi, and Beaverhead, 9) Flathead Fault, MT, 10) Bitterroot Fault, MT.

Intermountain Seismic Belt

Fault System	Priority	Segment	Swath Length (km	Swath Width (km)	Swath Area (km^2)	Total Area (km^2)	Comments
Wasatch Fault, Utah	1	Nephi Segment	17	1.5	25.5		Strike-parallel sections of segment
			8	2	16.0		
			7.5	1	7.5		
			7.2	1	7.2		
			8.1	1	8.1		
					64.3		Total area of south – north sections
			5	4	**20**		Area of rectangle on hanging wall
					85	85	***Total area of Nephi Fault Segment***
	1	Provo Segment	23	5	115		
			9	1	9		
			12	1	12		
			12	1	12		
			18	1.5	27		
			8	5	40		Provo – Salt Lake segment boundary
					215	215	***al area of Provo segment and segment boundary***
	1	Salt Lake Segment	8	1	8		South linear section
			12	1	12		Little Cot. To Big Cottonwood Canyon
			14	10	140		Salt Lake – Weber segment boundary
					160	160	***otal area for Salt Lake Segment & N. boundary***
	1	Weber Segment	32	2	64		
			24	3	72		
			4	15	60		Weber – Brigham City segment boundary
					196	196	***Total Weber Segment***
	1	Brigham City Segmen	28	1.5	**42**	42	***Total Brigham City Segment***
Mercur Fault (South)	2	Southern segment	20	4	80	80	
Stansbury Fault	2	Center scarps	5	3	15	15	
Cache Valley Faults	3	SW Fault	23	3	69		
	3	NW Fault	37	1	37		
			14	1	14		
			40	1.5	60		
			42	1	42		

					222	**222**	Total Cache Valley faults
Teton Fault, Wyoming	**1**		**45**	**4**	**180**		**Main fault zone in south**
			30	4	120		Main fault zone in north
			12	10	120		Signal Mountain boundary
					420	**420**	***Total Teton Fault***
Yellowstone Park	**1**	Profile South	50	1	50		
		Profile North	50	1	50		
		(Profiles aligned East-west)			**100**	**100**	***Total area in Yellowstone***
Madison Fault	**2**	Paritial length swath	20	1	**20**	**20**	
Central Idaho							
Lost River Fault	**1**	Partial length swath	20	1	20		
Lemhi Fault	**1**	Partial length swath	20	1	20		
Beaverhead Fault	**1**	Partial length swath	20	1	20		
					60	**60**	
Bitteroot Fault	**1**	Partial length swath	40	1	**40**	**40**	
Flat Head Fault	**1**	Partial length swath	40	1	**40**	**40**	
.ewis and Clark Shear Zon	**1**	Selected Segments	155	1	**155**	**155**	

Area for all priorities 1860 km^2
Priority 1 Area: 1513
Priority 2 Area: 115
Priority 3 Area: 222

Cascadia

Overview of Region

The Cascadia plate boundary has characteristics that lead to a modification of the LiDAR acquisition strategy used in most of the other regions. Much of the near surface deformation associated with plate interactions occurs off-shore within the accretionary wedge, and thus is not accessible by LiDAR. Additionally several previous LiDAR projects have obtained substantial imagery in the highly populated Puget Sound and Portland (Oregon) regions. As a result, the GeoEarthScope LiDAR acquisition is targeted at 3 locations within the Cascadia system at sites where onshore deformation associated with the plate interactions can be imaged (see Figure 4, Table 5). The three sites are (1) The southern termination of the Cascadia margin in northern California in the vicinity of Eureka; (2) the Calawah Fault in the deforming forearc on the western Olympic Peninsula; and (3) the Yakima Fold belt on the east side of the Cascade Range. Each of these sites provides an opportunity to obtain key information on subduction related deformation as described below.

Details of the Fault System

Mendocino Triple Junction (MTJ) Region: In the vicinity of the MTJ, the Cascadia subduction zone is converted to the translational San Andreas plate boundary. In this region, the convergent deformation and associated faults come onshore and are targets for LiDAR. Two fault zones are identified as Priority 1 targets (Fig. 4) – the Mad River Fault zone and the Little Salmon Fault. Both are complex faults with both convergent and translational deformation and reflect the tectonic processes in the transition from subduction to translation. Additionally these faults are the onshore continuations of the offshore subduction deformation. Slip rates on these faults are uncertain but are estimated to potentially be in the 5 mm/yr range and thus reflect a significant component of the Cascadia deformation.

The Mad River and Little Salmon Faults also in a sense reflect the northernmost extent of the San Andreas plate boundary. Although the linkage between these two segments of the North America plate boundary is not well understood. LiDAR imagery on these faults in concert with that obtained for Northern California will provide an important data set to improve our understanding of the links between Cascadia and the San Andreas.

The Mad River fault zone requires a relatively broad swath and thus we propose a 10 km wide by 30 km long swath imaging this fault zone running SE from the coast. The Little Salmon fault can be imaged with a 2-km wide swath and thus a 50 km length of that fault is proposed. Both are proposed as Priority 1 targets.

Calawah Fault: The Calawah fault in northwestern Washington reflects forearc-block motion within the Cascadia subduction margin, specifically differential motion between the Olympic Mountains and Vancouver Island blocks. Kinematic, geodetic, and geologic observations suggest up to 3.5 mm/y of north-south contraction between the Olympic Mountains and Vancouver Island, accommodated by a combination of distributed uplift in the Olympic Mountains and faulting along the block boundary (Figure XX). The tide gauge at Neah Bay

records one of the highest rates of uplift along the Cascadia subduction margin, and uplift rates derived from repeated leveling surveys depict a sharp gradient across the Calawah fault. The Calawah fault, which marks the modern boundary between terranes, is a prime candidate for carrying a significant portion (~1-2 mm/y) of this relative motion.

Geomorphology in the vicinity of the Calawah fault suggests a significant component of left-lateral strike-slip motion as well as vertical motion. In particular, stream courses are offset across the fault, some stream channels have been abandoned (denoted by orange lines) or blocked, diverting stream courses into circuitous routes. Offshore in Makah Bay, multibeam, sidescan-sonar, and high-resolution seismic reflection data image a fault zone that offsets the sea floor and may serve to shift Cape Flattery left laterally (*i.e.*, seaward). NOAA-OCNMS has already collected high resolution multi-beam bathymetry along the Calawah fault in Makah Bay as well as LIDAR along the shoreline and is interested in merging their offshore data sets with new onshore data, to yield a unique integrated map of an onshore-offshore fault system. Approximately 100 km^2 of LiDAR acquisition is proposed for the Calawah Fault.

Yakima Fold Belt: The Yakima Fold belt reflects the Cascadia associated deformation that is occurring relatively far-field from the subduction front. We propose a small (~ 50km^2) LiDAR survey in the fold belt to assess the style of deformation and the potential for GeoEarthScope relevant data in the convergent plate boundary hinterland.

Table 5 – Cascadia LiDAR Targets

Region	*Fault*	*Priority*	*LiDAR (km^2)*
MTJ			
	Mad River Fault Zone	1	300
	Little Salmon Fault	1	100
Fore-Arc			
	Calawah Fault	1	100
Back-Arc			
	Yakima Fold Belt	1	50
Total			***550 km^2***

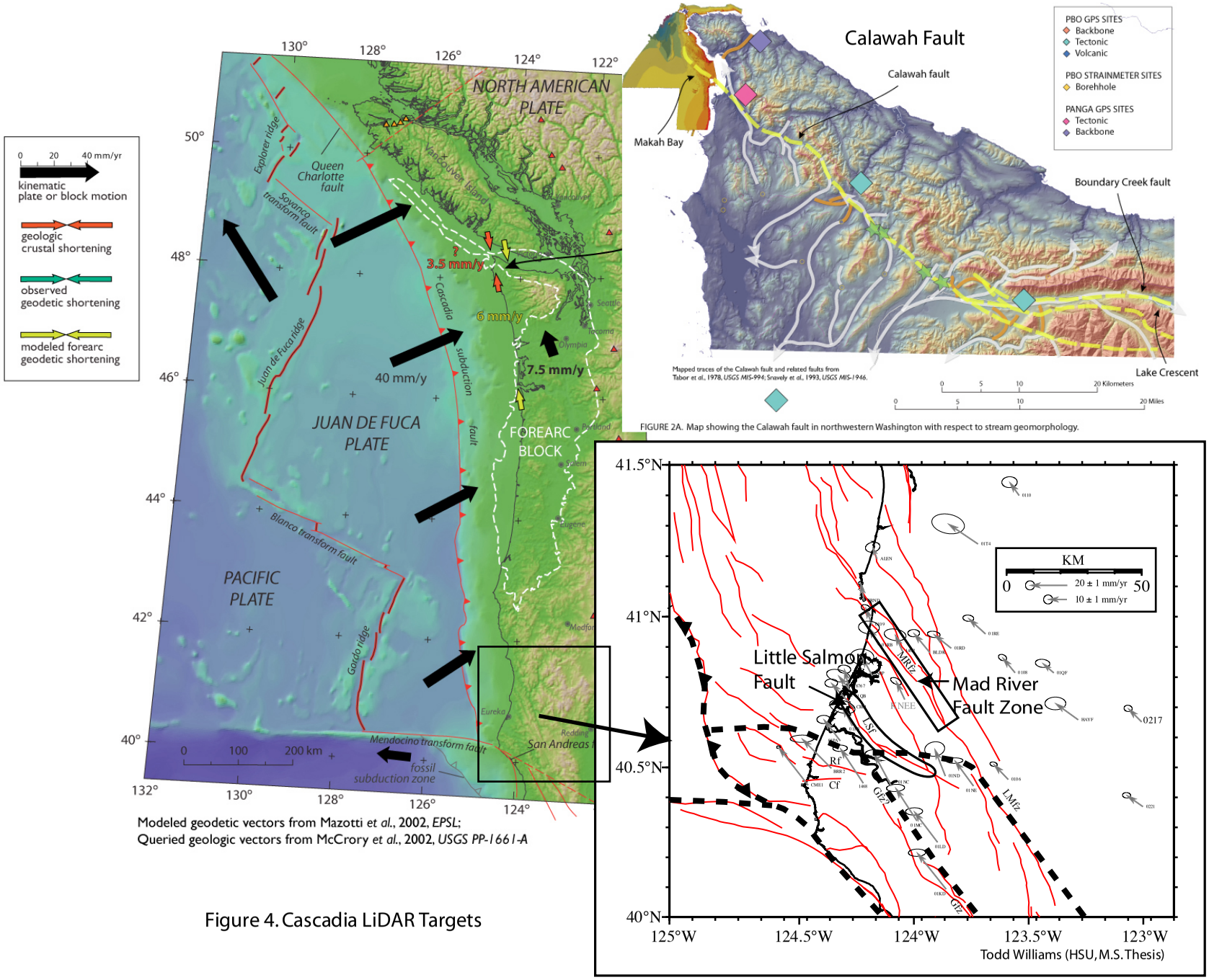

FIGURE 2A. Map showing the Calawah fault in northwestern Washington with respect to stream geomorphology.

Figure 4. Cascadia LiDAR Targets

Alaska

Overview

Targets for LiDAR acquisition in Alaska focus on the Castle Mountain Fault, the Denali Fault, and deformed river terraces located on the north flank of the Alaska Range (Fig. 5). The Castle Mountain fault is a regional strike-slip fault with approximately 60 km of Holocene scarps that is located within the Greater Anchorage region, the most urbanized and rapidly developing area in the state of Alaska. The Denali Fault is one of the world's great intra-continental strike-slip fault systems that extend for over 1500 km through Canada and interior Alaska. The Nenana River heads on the south side of the Alaska Range and flows northward crossing the Denali Fault and the northern flank of the Alaska Range before joining the Tanana River in interior Alaska. Sequences of Pliocene and Quaternary river terraces preserved along the course of the Nenana River provide a record of the uplift and propagation of the Alaska Range during the last 5 Ma. Flights of variably tilted terraces along the Nenana River provide a spectacular target for LiDAR.

Geological Synopsis

Alaska is the most seismically active region in the United States because of plate interactions that include transform faulting, plate subduction, and microplate collision (Plafker and Berg, 1994a; Page *et al.*, 1991). The state contains the highest point in North America at 20,300+' elevation at Mount McKinley, and one of the most spectacular coastal mountains belts on earth where the Saint Elias Mountains are forming in response to collision of the Yakutat microplate in the transition from transform faulting along the Fairweather Fault to subduction and accretion at the northeastern end of the Aleutian trench (e.g., Bruhn et al., 2004). The coastal and interior mountains are young, with much of the contemporary topography evolving in the last 5 Ma because of low-angle subduction and accretion of the Yakutat microplate. This includes uplift of the Alaska Range hundreds of kilometers from the plate margin, as well as uplift of the Saint Elias coastal mountains. Farther west, subduction of the Pacific Plate creates the Alaska-Aleutian volcanic arc where there are scores of active volcanoes and frequent large to great magnitude earthquakes (Fig. 5).

The state of Alaska is constantly rocked by large to great magnitude earthquakes (Fig 5; Haeussler and Plafker map; Plafker *et al.*, 1994b). Some recent examples include the 1958 M 7.9 earthquake on the Fairweather transform fault, the 1964 Great Alaskan earthquake (M 9.2) which ruptured the eastern part of the Aleutian megathrust, and the recent 2002 Denali Fault earthquake (M 7.9) which ruptured for a length of about 350 km through the interior of the Alaska Range (Fig. 5). Rates of tectonic motion are also significant; transform faulting and subduction along the plate margin ranges from 50 to 60 mm/yr. In interior Alaska the Denali fault slips at approximately 10 mm/yr. The Castle Mountain fault in the Greater Anchorage area slips at a rate of roughly 3 mm/yr, and generated four M 6.5 – 7 surface rupturing earthquakes in the last 2800 years, with a similar recurrence interval to M 9+ earthquakes that occur on the underlying subduction megathrust (Haeussler et al, 2002).

Research Impacts

Alaska is the premier place in the United States to study plate margin and intra-continental deformation driven by subduction and microplate collision. The latter process is of global significance because most mountain belts are formed largely by the collision and accretion of plate fragments over time. In Alaska, we are just learning how profound such collisions can be – low-angle subduction of the Yakutat microplate is now thought to drive active deformation far into the interior of the North American plate, over distances of 1000 km inland!

Geological Hazards

Although the population density of Alaska remains small compared to much of the United States there is significant risk to people and infrastructure. The Greater Anchorage area is the most populated part the state and is subject to great earthquakes on the underlying subduction zone. There is also the potential for damaging earthquakes generated on shallow crustal faults, including fault-cored folds in Cook Inlet Basin, and the Castle Mountain Fault (Fig. 5) (Haeussler *et al*., 2000). There is also much to be learned about seismic hazards.

Recent work by Willis et al. determined that the slip-rate on the Castle Mountain Fault is roughly 3 mm/yr, almost twice that estimated previously when compiling the seismic hazard map of Alaska (Wesson *et al*., 1999; Wesson *et al*., in press). This right-lateral strike-slip fault is capable of generating M 7 earthquakes in close proximity to Anchorage and surrounding towns, and has apparently done so at least four times in the last 2800 years (Haeussler *et al*., 2002). The slip-rate estimated by Willis et al. (under review) is averaged over the last 11 – 13 Ka. High resolution LiDAR acquisition along the 60 km length of Holocene surface rupture will undoubtedly reveal a number of offset features that will allow paleoseismologists to further refine the slip-rate and recurrence interval of surface rupturing earthquakes (Fig. 5). Interpretation of a seismic line across the fault suggests the presence of an anticline, cored by blind thrusts that sole into the Castle Mountain fault on its northwest side (Haeussler *et al*., 2000). The thrust faults potentially could: (1) slip and initiate rupture on the Castle Mountain Fault just as slip on the Susitna Glacier thrust fault initiated the 2002 Denali fault earthquake (Eberhart-Phillips *et al*., 2003); (2) slip independently of the Castle Mountain Fault; or (3) slip shortly after a rupture on the Castle Mountain Fault. The blind thrust faults thus increase the seismic hazards along the Castle Mountain Fault; and a goal of LiDAR data interpretation along the fault will be to carefully scrutinize for geomorphic expressions of the anticline and blind thrust faults.

The Alaska Range is a spectacular mountain belt created largely in the last 5 Ma by transpressional deformation along the Denali fault system (Fig. 1), which is partly driven by counter-clockwise rotation of the Southern Alaska Block, a large continental tectonic block that is at least partly driven by low-angle subduction of the Yakutat microplate. Transpression along the central and western part of the Denali fault created the highest peaks of the Alaska Range during the last 5 Ma, including Mt. McKinley in Denali National Park. The Denali Fault is similar in length to the San Andreas fault of California, and the recent 2002 rupture of the Denali Fault during an M 7.9 earthquake is an important analog for the expected future 'big one' along the San Andreas Fault. Subsequent to the 2002 earthquake, paleoseismology and landslide studies of the Denali Fault have produced new and important information on earthquake

recurrence patterns, rupture behavior within fault segments, and also on strong ground motion associated with strike-slip faulting. LiDAR surveys along the parts of the trace of the Denali fault hold the potential to further reveal information on late Pleistocene and Holocene rupture history, fault slip-rate and displacement patterns, and partitioning of deformation between strike-slip and thrust faulting where transpression increases from east to west along the length of the fault. The Denali Fault rupture initiated on the previously unknown Susitna Glacier thrust fault which is located in a confining bend of the Denali Fault. A LiDAR swath along the thrust fault may be included in a survey of the Denali Fault to examine previously unnoticed geomorphic expressions of the fault (incised streams and terraces that were observed in the field but due to inaccessibility have not been analyzed) and interactions between the thrust fault and the strike-slip fault. Approximately 350 square kilometer of LiDAR surveying are proposed along this Denali Fault, with swaths located in regions that are free of glacier ice. Only the general areas of interest are shown in Figure 1; detailed swath segments will need to be defined.

Flights of river terraces preserved along the course of the Nenana River provide a unique opportunity to study the timing and spatial distribution of uplift associated with thrust faulting and folding in the northern flanks of the Alaska Range. We propose at least a 50 km x 2 km LiDAR swath over these terraces (Fig. 5). The combined studies of the Denali fault and foreland fold and thrust belt will be of considerable interest to the public at large because of proximity to Denali National Park, in addition to the purely scientific merits. Notably, this region is also located near the Alaska Range crossing of the TransAlaska oil pipeline, and is also a probable location for a proposed new gas pipeline that will bring North Slope and Brooks Range gas southward for distribution into Canada, southern Alaska and the continental US.

Table 6 – Alaska LiDAR Targets

LiDAR Target	***Swath Length***	***Swath Width***	***Comments***
Castle Mountain Fault	60 km	1 – 1.5 km	Seismic Hazard to Urban Area
Denali Fault	350 km	1 km average	Basic science of strike-slip faulting
Nenana River Terraces	50 km	2 km	Foreland fold and thrust belt
			Total Area: about 500 km^2

- Notes on Denali Fault – part of fault is buried beneath glaciers; the survey also, may extend onto the Totschunda Fault and the Susitna Glacier thrust fault, both of which ruptured as part of the 2002 M 7.9 Denali Fault earthquake.

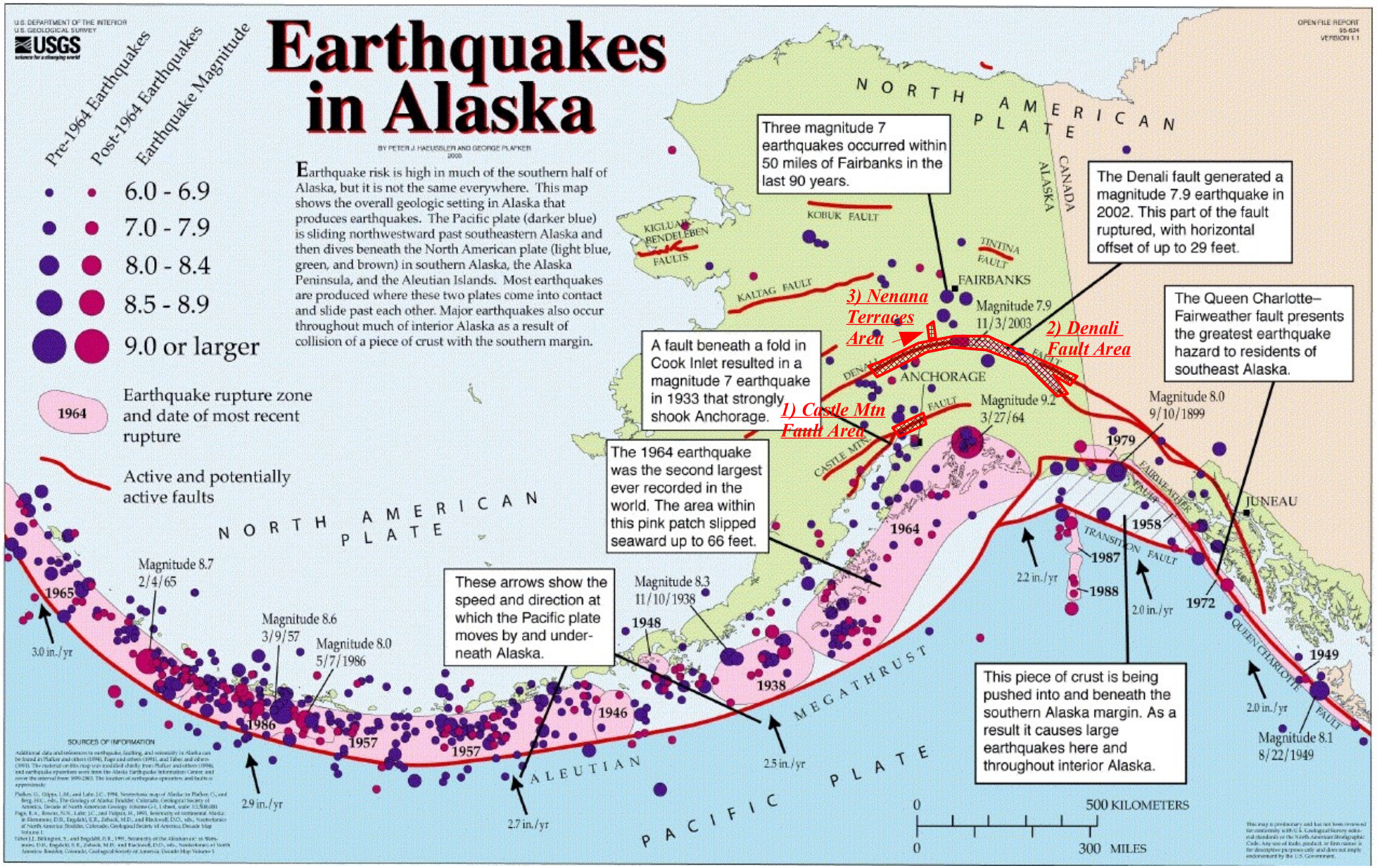
U.S. DEPARTMENT OF THE INTERIOR
U.S. GEOLOGICAL SURVEY
USGS
OPEN FILE REPORT
95-624
VERSION 1.1
Earthquakes in Alaska
BY PETER J. HAEUSSLER AND GEORGE PLAFKER
2000
Earthquake risk is high in much of the southern half of Alaska, but it is not the same everywhere. This map shows the overall geologic setting in Alaska that produces earthquakes. The Pacific plate (darker blue) is sliding northwestward past southeastern Alaska and then dives beneath the North American plate (light blue, green, and brown) in southern Alaska, the Alaska Peninsula, and the Aleutian Islands. Most earthquakes are produced where these two plates come into contact and slide past each other. Major earthquakes also occur throughout much of interior Alaska as a result of collision of a piece of crust with the southern margin.
Pre-1964 Earthquakes
Post-1964 Earthquakes
Earthquake Magnitude
6.0 - 6.9
7.0 - 7.9
8.0 - 8.4
8.5 - 8.9
9.0 or larger
1964
Earthquake rupture zone and date of most recent rupture
Active and potentially active faults
NORTH AMERICAN PLATE
PACIFIC PLATE
ALEUTIAN MEGATHRUST
ALASKA
CANADA
Three magnitude 7 earthquakes occurred within 50 miles of Fairbanks in the last 90 years.
The Denali fault generated a magnitude 7.9 earthquake in 2002. This part of the fault ruptured, with horizontal offset of up to 29 feet.
The Queen Charlotte–Fairweather fault presents the greatest earthquake hazard to residents of southeast Alaska.
A fault beneath a fold in Cook Inlet resulted in a magnitude 7 earthquake in 1933 that strongly shook Anchorage.
The 1964 earthquake was the second largest ever recorded in the world. The area within this pink patch slipped seaward up to 66 feet.
These arrows show the speed and direction at which the Pacific plate moves by and underneath Alaska.
This piece of crust is being pushed into and beneath the southern Alaska margin. As a result it causes large earthquakes here and throughout interior Alaska.
KOBUK FAULT
KIGLUAIK
BENDELEBEN
FAULTS
TINTINA FAULT
KALTAG FAULT
FAIRBANKS
Magnitude 7.9
11/3/2003
3) Nenana Terraces Area
2) Denali Fault Area
1) Castle Mtn Fault Area
ANCHORAGE
DENALI FAULT
CASTLE MTN. FAULT
Magnitude 9.2
3/27/64
Magnitude 8.0
9/10/1899
1979
FAIRWEATHER FAULT
JUNEAU
1958
TRANSITION FAULT
1987
1988
1972
QUEEN CHARLOTTE FAULT
1949
Magnitude 8.1
8/22/1949
1964
1965
Magnitude 8.7
2/4/65
Magnitude 8.6
3/9/57
Magnitude 8.0
5/7/1986
1986
1957
1957
1946
1948
Magnitude 8.3
11/10/1938
1938
3.0 in./yr
2.9 in./yr
2.7 in./yr
2.5 in./yr
2.2 in./yr
2.0 in./yr
2.0 in./yr
0
500 KILOMETERS
0
300 MILES
SOURCES OF INFORMATION